doi:10.1016/j.jmb.2007.11.050 J. Mol. Biol. (2008) 375, 1206–1211

JMB

Available online at www.sciencedirect.com

ScienceDirect

ELSEVIER

COMMUNICATION

Trapping of a Transcription Complex Using a New Nucleotide Analogue: AMP Aluminium Fluoride

Nicolas Joly[1]†, Mathieu Rappas[2]†, Martin Buck[1]* and Xiaodong Zhang[2]*

[1]*Division of Biology, Sir Alexander Fleming Building, Imperial College London, Exhibition Road, South Kensington, London SW7 2AZ, UK*

[2]*Division of Molecular Biosciences, Biochemistry Building, Imperial College London, Exhibition Road, South Kensington, London SW7 2AZ, UK*

Received 24 September 2007; received in revised form 14 November 2007; accepted 15 November 2007
Available online 22 November 2007

Edited by K. Morikawa

Mechanochemical proteins rely on ATP hydrolysis to establish the different functional states required for their biological output. Studying the transient functional intermediate states these proteins adopt as they progress through the ATP hydrolysis cycle is key to understanding the molecular basis of their mechanism. Many of these intermediates have been successfully 'trapped' and functionally characterised using ATP analogues. Here, we present a new nucleotide analogue, AMP–AlF_x, which traps PspF, a bacterial enhancer binding protein, in a stable complex with the σ^{54}-RNA polymerase holoenzyme. The crystal structure of AMP–AlF_x•$PspF_{1–275}$ provides new information on protein–nucleotide interactions and suggests that the β and γ phosphates are more important than the α phosphate in terms of sensing nucleotide bound states. In addition, functional data obtained with AMP–AlF_x establish distinct roles for the conserved catalytic AAA^+ (ATPases associated with various cellular activities) residues, suggesting that AMP–AlF_x is a powerful new tool to study AAA^+ protein family members and, more generally, Walker motif ATPases.

Keywords: AAA^+ ATPase; nucleotide analogue; transcription; bEBP; PspF

In bacteria, the major variant sigma factor, sigma54 (σ^{54}), forms a transcriptionally silent closed complex with RNA polymerase (E) at σ^{54}-dependent promoters. ATP hydrolysis by a σ^{54} activator protein that belongs to the large AAA^+ (ATPases associated with various cellular activities) protein family is required to actively remodel the closed complex to a transcriptionally competent open complex.[1–3] σ^{54} activators are also termed bacterial enhancer binding proteins (bEBPs)[4] as they often bind upstream activating sequences located approximately 100 bp upstream from the σ^{54} promoter. bEBPs, like most AAA^+ proteins, first need to oligomerise (usually to form hexamers) to be functionally active. What distinguishes bEBPs from other AAA^+ family members is the presence of a highly conserved GAFTGA motif, shown to be essential for σ^{54} binding, found at the tip of the L1 loop.[5–9] Structurally characterised bEBPs include NtrC1, PspF, ZraR and NtrC.[7–10] The AAA^+ domains of NtrC1 and PspF form functionally relevant stable complexes with σ^{54} or $E\sigma^{54}$ in the presence of the nucleotide analogues ADP–BeF_x and ADP–AlF_x thought to mimic the ATP-bound state prior to, or at the point of, ATP hydrolysis, respectively.[8–13] The complexes formed using these nucleotide analogues have been proposed to closely represent otherwise transient intermediates formed with ATP. However, the precise number and arrangement of the fluoride ions in the AlF_x or BeF_x moieties within the nucleotide-binding pockets of these bEBPs remains unknown, making the exact assignment of the respective complexes to the different nucleotide states (ground or transition state) somewhat uncertain. We previously proposed that sensing the nucleotide-bound state of PspF involves the Walker B residue E108 and that *via* its interaction with residue N64 the ATP can affect the conformation of the σ^{54} interacting L1 loop.[14] We

**Corresponding authors.* E-mail addresses: m.buck@imperial.ac.uk; xiaodong.zhang@imperial.ac.uk.

† N.J. and M.R. contributed equally to this work.

Abbreviations used: AAA^+, ATPases associated with various cellular activities; bEBP, bacterial enhancer binding proteins; WT, wild type.

proposed that in the ADP-bound state the L1 loop is locked in a nonproductive conformation, unable to interact with σ^{54}. Upon ATP binding, an interaction between E108 and N64 promotes the release of the L1 loop, enabling the interaction with σ^{54} to take place.[12,14] At the point of ATP hydrolysis, the L1 loop is further exposed, allowing more stable interactions with σ^{54} to occur.

Nucleotide analogues are routinely used to capture proteins in transient conformational states; they are thus indispensable tools to successfully study and dissect the different stages of nucleotide hydrolysis-driven molecular mechanisms. Here, we report the identification and functional characterisation of a new stable complex between the AAA$^+$ domain of PspF (residues 1 to 275, hereinafter called PspF$_{1–275}$) and σ^{54} or Eσ^{54} using the new nucleotide analogue AMP–AlF$_x$ formed *in situ*. In addition, using site-directed mutagenesis and biochemical approaches, we assign the residues in PspF$_{1–275}$ that are responsible for forming either the ADP–AlF$_x$- or the AMP–AlF$_x$-dependent complexes. Detailed analysis of our data suggests that the highly conserved AAA$^+$ catalytic residues, including the Walker B motif residues and the putative arginine finger (R finger) residues, have distinct roles in catalysis and may therefore be implicated in PspF functionality at different stages of the hydrolysis cycle.

AMP–AlF$_x$ complex formation

To investigate whether nucleotide analogues other than ADP–AlF$_x$ support formation of stable complexes between the activator protein and σ^{54} or Eσ^{54}, we performed 'trapping experiments' as described in Refs. 11,15 in which we replaced ADP with AMP. Incubation of PspF$_{1–275}$ wild type (WT) with σ^{54} or Eσ^{54} in the presence of AMP, $AlCl_3$ and NaF led to formation of stable AMP–AlF$_x$•PspF$_{1–275}$WT•σ^{54} or AMP–AlF$_x$•PspF$_{1–275}$WT•Eσ^{54} complexes, which migrate with the same mobility as ADP–AlF$_x$-dependent complexes on native gels, suggesting that they are very similar (Fig. 1a, lanes 2, 3, 8 and 9). As a control, we demonstrated that AMP alone did not support formation of stable complexes between PspF$_{1–275}$ and σ^{54} (or Eσ^{54}) (Fig. 1a, lanes 4–6). Interestingly, we noted that when using the histidine-tagged form of PspF$_{1–275}$WT [(His)$_6$-PspF$_{1–275}$WT] we observed a stable homohexamer of (His)$_6$-PspF$_{1–275}$WT in the presence of ADP–AlF$_x$ but not AMP–AlF$_x$, suggesting differences between PspF$_{1–275}$WT subunits exist in the presence of these two nucleotide analogues (Table 1).

AMP–AlF$_x$ trapped complex characterisation

To further characterise the new AMP–AlF$_x$•PspF$_{1–275}$•σ^{54} (or Eσ^{54}) complex, we performed gel filtration experiments. Elution profiles of the PspF$_{1–275}$•σ^{54} complexes obtained using either ADP–AlF$_x$ or AMP–AlF$_x$ are very similar (Fig. 1b). We thus conclude from the gel filtration and band shift assays that the ADP–AlF$_x$- and AMP–AlF$_x$-dependent complexes are similar in terms of size and stability. In addition, DNA-binding assays, using fluorescent probes mimicking different promoter DNA conformations,[17] demonstrated no significant

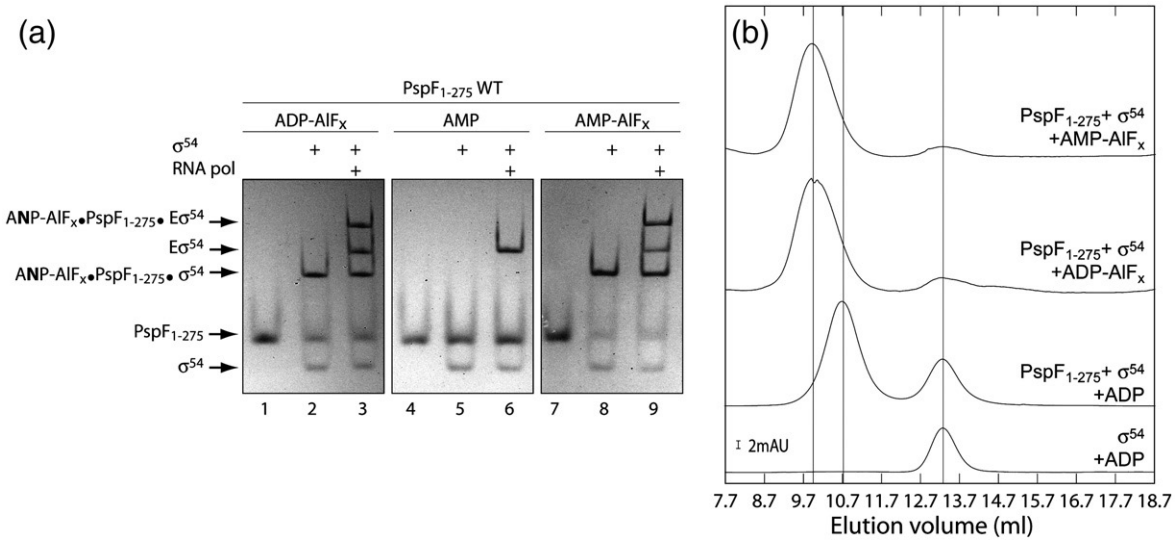

Fig. 1. Identification and characterisation of new stable PspF$_{1–275}$ WT•σ^{54} or Eσ^{54} complexes in the presence of AMP–AlF$_x$. (a) Native gel showing the complexes formed by PspF$_{1–275}$ WT (5 μM) with or without σ^{54} (1 μM) and with or without RNA polymerase (0.15 μM) in the presence of AlF$_x$ reactant [AlC_3 (0.4 mM) + NaF (5 mM)] and different nucleotides (4 mM, as indicated). The sample was loaded onto native 4.5% PAGE and proteins were detected by Coomassie blue staining. ANP indicates AMP or ADP. (b) Gel filtration profiles of samples containing PspF$_{1–275}$ WT (64 μM) with or without σ^{54} (30 μM) and with or without AMP–AlF$_x$ or ADP–AlF$_x$ (as indicated) chromatographed through a Superdex 200 column (10 mm × 300 mm, 24 ml, GE Healthcare) at 4 °C. The scale bars give the scale of the ordinate axis; absorption units (AU) correspond to an $A_{280\ nm}$ of 1.

Table 1. Summary of the native gel analysis demonstrating whether trapped complexes were obtained using $PspF_{1–275}$ variants and different nucleotides in the presence of $AlCl_3$ and NaF

$PspF_{1–275}$	Nucleotide + $AlCl_3$ + NaF	Alone	σ^{54}	$E\sigma^{54}$
His-WT	ADP	+	+	+
	ATP	+	+	+
	AMPPNP	–	–	–
	AMP	–	+	+
WT	ADP	–	+	+
	ATP	–	+	+
	AMPPNP	–	–	–
	AMP	–	+	+
K42A	ADP	–	–	–
	ATP	–	–	–
	AMPPNP	–	–	–
	AMP	–	–	–
L44A	ADP	–	–	–
	ATP	–	–	–
	AMPPNP	–	–	–
	AMP	–	–	–
D107A	ADP	–	+	+
	ATP	–	–	–
	AMPPNP	–	–	–
	AMP	–	–	–
E108A	ADP	–	–	–
	ATP	–	+*	+*
	AMPPNP	–	–	–
	AMP	–	–	–
R162A	ADP	–	+	+
	ATP	–	–	–
	AMPPNP	–	–	–
	AMP	–	–	–
R168A	ADP	–	–	–
	ATP	–	–	–
	AMPPNP	–	–	–
	AMP	–	–	–

'–', no complex observed on native gel; '+', complex observed on native gel; '+*', complex observed on native gel but not dependent on $AlCl_3$ + NaF.[16]

differences in the DNA-binding properties of the two types of 'trapped' complexes (data not shown). Having established that the AMP–AlF$_x$-dependent complexes can bind DNA, we investigated whether the AMP–AlF$_x$•$PspF_{1–275}$•$E\sigma^{54}$ complex was able to activate transcription *in vitro* from the supercoiled *Sinorhizobium meliloti nifH* promoter. Similar to the ADP–AlF$_x$•$PspF_{1–275}$•$E\sigma^{54}$ complex, transcription from the AMP–AlF$_x$•$PspF_{1–275}$•$E\sigma^{54}$ complex was not observed (data not shown). Finally, using in-solution DNA cross-linking (as described in Ref. 16), we found no significant differences between the ADP–AlF$_x$- and AMP–AlF$_x$-dependent complexes formed with σ^{54}, suggesting that the protein·DNA interactions are similar when using the two AlF$_x$-dependent nucleotide analogues (P. Burrows and N. Joly, unpublished result).

Taken together, these results indicate that both AMP–AlF$_x$- and ADP–AlF$_x$-dependent complexes are likely to have similar conformations and stability, although some subtle differences do exist.

Structure of Mg-AMP-bound $PspF_{1–275}$

To establish the detailed organisation of Mg-AMP–AlF$_x$-bound $PspF_{1–275}$, and to provide a structural basis for the distinct determinants implicated in forming ADP–AlF$_x$ *versus* AMP–AlF$_x$ complexes, we soaked $PspF_{1–275}$ crystals with $MgCl_2$, AMP, $AlCl_3$ and NaF (Table 2). These crystals diffracted to 2.85 Å at the European Synchrotron Radiation Facility (ESRF) and the structure was solved by molecular replacement using the structure of apo $PspF_{1–275}$ WT as a search model. Inspection of the first $F_o - F_c$ map contoured at 3σ revealed clear densities for both the AMP and the Mg moieties and an extra density located at the tip of the α phosphate of the AMP moiety (Fig. 2a), which is too large to be a water molecule. We believe this density corresponds to the AlF$_x$ moiety, but because of the low resolution we cannot establish this unambiguously and are thus unable to conclude anything regarding the precise coordination of the Al ion. The structure, however, clearly shows that the torsion angles around the ribose moiety and the phosphate backbone have significantly changed when compared with those in either the AMPPNP-, ATP- or ADP-bound structures.[14] The torsion angle of the C_4'–C_5' bond changes 114°, from 38° in the ATP-bound structure to 152° in the Mg-AMP-bound structure, and as a result the ribose plane is translated some 3 Å towards the Walker B motif, allowing the α phosphate of AMP to occupy the canonical position of the β phosphate of ATP (Fig. 2). The extra electron density (potentially the AlF$_x$ moiety) occupies a position similar to that of the γ phosphate of ATP in the ATP-bound structure

Table 2. Crystallographic data and refinement statistics of Mg-AMP-bound $PspF_{1–275}$

Structure	Mg-AMP-$PspF_{1–275}$
Space group	$P6_5$
Unit cell (Å)	$a = b = 113.6$; $c = 39.3$; $\alpha = \beta = 90°$; $\gamma = 120$
A. *Data reduction statistics*	
λ (A)	0.97570
Resolution (Å)	98.39–2.85 (3.0–2.85)
Unique reflections	6998
Redundancy	10.4 (10.7)
I/σ	4.7 (1.9)
I, mean (SD)	18.2 (6.5)
Completeness (%)	100 (100)
R_{meas} (%)	14.3 (38.3)
R_{pim} (%)	4.4 (11.6)
R_{sym} (%)	13.6 (36.4)
B. *Refinement statistics*	
Reflections (work/free)	6985/348
No. of atoms	2093 (114 water molecules)
R_{work} (%)	18.6
R_{free} (%)	24.1
Ramachandran plot (%)	
Favoured regions	90.1
Additional allowed regions	9.4
Generously allowed regions	0.5
Disallowed	0
RMSD from ideality	
Bond lengths (Å)	0.013
Bond angles (°)	1.4

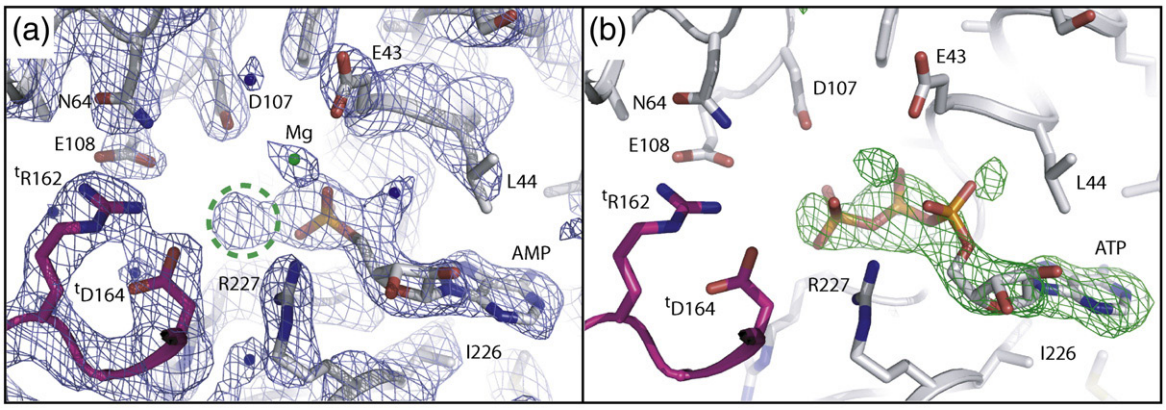

Fig. 2. Final $2F_o - F_c$ and omit difference $F_o - F_c$ electron density maps of the nucleotide-binding pocket of PspF$_{1–275}$. (a) Final $2F_o - F_c$ map of the Mg-AMP-PspF$_{1–275}$ structure at 2.85 Å resolution contoured at 1σ. The neighbouring subunit is coloured magenta. Important intramolecular catalytic residues are highlighted and important intermolecular catalytic residues offered by the neighbouring subunit are denoted 't' for 'trans'. Note how the extra electron density encircled in green dashed lines occupies the position of the γ phosphate in ATP-bound structures of PspF$_{1–275}$ and is connected to the electron density of the AMP moiety. (b) Omit difference $F_o - F_c$ map of the Mg-AMP-PspF$_{1–275}$ structure contoured at 3σ. The PspF$_{1–275}$-ATP-bound structure was superimposed onto the P loop of the PspF$_{1–275}$-Mg-AMP-bound structure and the result is displayed in this figure. Note that ATP fits convincingly into the difference map. Further note how the γ phosphate of ATP fits into the extra density encircled in (a). Data were collected at ESRF beamline ID-29. Refinement of the structure was performed as described[14] and the nucleotide and the Mg ion were refined with unit occupancy. Map inspection, model building and water molecule picking were done using Coot.[18] The average temperature factors in this structure are 30 for the protein, 60 for the AMP and 57 for the Mg. For analysis, all the liganded (ATP: 2C96; ADP: 2C98; AMPPNP: 2C99; Mg-ATP-PspF$_{1–275}$R227A: 2C9C) and unliganded (Apo: 2BJW) PspF structures were aligned onto their P loops (residues 35 to 43). All figures were prepared using Pymol (Delano, W. L. (2002). *The PyMOL Molecular Graphics System* on the World Wide Web, http://www.pymol.org).

(Fig. 2).[14] We also observe a water molecule sitting where the apical oxygen of the α phosphate of ATP lies in the ATP-bound structure (Fig. 2).[14] Interestingly, the N-terminus of PspF appears more structured and has moved 0.5 Å towards the Walker B motif when compared to the ATP-bound structure. This movement of the N-terminus could promote or facilitate the translation of AMP to compensate for the missing β phosphate.

When superposing the ATP-bound structure onto the Mg-AMP-bound structure, ATP fits convincingly into the $F_o - F_c$ difference map contoured at 3σ (Fig. 2b). We note that the α phosphate of ATP lies outside the density, whereas the β phosphate and γ phosphate fit inside it. This observation suggests that the AMP–AlF$_x$ analogue, regardless of the coordination of the Al, mimics more closely a triphosphate nucleoside rather than a diphosphate one. Furthermore, when comparing the Mg-AMP-bound structure to the AMPPNP-, Mg-ATP- and ADP-bound structures[14] we notice that certain key residues and secondary structure elements adopt conformations that are closer to those previously observed in the triphosphate nucleoside-bound structures. Indeed, the crucial Walker B E108 residue adopts in the Mg-AMP-bound structure a conformation midway between that observed in the AMPPNP-bound structure and that observed in the Mg-ATP-bound structure. In addition, the L1 loop in the Mg-AMP-bound structure is as ordered and points in the same direction as in the AMPPNP-bound structure. The L1 loop is not as disordered as in the Mg-ATP-bound structure and it points up instead of pointing down as it does in the ADP-bound structure. Finally, in the Mg-AMP-bound structure the N-terminus of PspF appears more structured and has moved 0.5 Å towards the Walker B motif when compared to the N-terminus in the Mg-ATP-bound structure and 1.2 Å when compared to the ADP-bound structure. This movement of the N-terminus could promote or facilitate the translation of the AMP to compensate for the missing β phosphate.

Translation of the AMP is consistent with results using the human guanylate binding protein 1, which showed a clear diphosphatase activity, and revealed that GMP-AlF$_4$ adopts a conformation that permits the AlF$_4$ moiety to occupy the canonical position of the γ phosphate of guanosine 5′-triphosphate.[19] Interestingly, for hydrolysis of guanosine 5′-diphosphate (GDP) to occur, the GDP moiety has to be translated in the binding pocket, and the torsion angle between the ribose moiety and the phosphate backbone needs to change so that the β phosphate of GDP occupies the canonical position of the γ phosphate of guanosine 5′-triphosphate, whilst the α phosphate occupies that of the β phosphate, similar to the Mg-AMP-bound structure presented here (Fig. 2). We did not detect hydrolysis of ATP (or ADP) to AMP by PspF$_{1–275}$.

Determinants for ADP–AlF$_x$ *versus* AMP–AlF$_x$ complex formation

In order to better understand the organisation of AMP and ADP within AlF$_x$-containing complexes

and to probe any intrinsic differences between these two complexes, we chose to mutate residues implicated in ATP binding and hydrolysis. More specifically, residues that contact the γ phosphate and the β phosphate of ATP, as well as the potential 'trans' (provided by the neighbouring subunit) R finger residues involved in intersubunit ATP hydrolysis were substituted using site-directed mutagenesis. Using the same experimental approach as described in Fig. 1a, we screened for complexes formed with PspF$_{1–275}$ variants. Two distinct classes of residues emerged: (i) residues required for forming both ADP–AlF$_x$- and AMP–AlF$_x$-dependent complexes and (ii) residues essential only for AMP–AlF$_x$-dependent complex formation.

Residues implicated in both ADP–AlF$_x$- and AMP–AlF$_x$-dependent complex formation include the Walker A residue K42, the ribose-interacting residue L44, the Walker B residue E108 and the trans R finger residue R168 (^{t}R168) (Table 1). Substitution of these residues with alanine eliminated both ADP–AlF$_x$- and AMP–AlF$_x$-dependent complex formation. Specific determinants for AMP–AlF$_x$ complex formation are the Walker B D107 residue and the trans R finger residue R162 (^{t}R162) (Table 1).

The Walker B motif residues D107 and E108 and the R finger residues R162 and R168 are conserved features among AAA$^+$ proteins. They are categorized as catalytic residues since their substitution results in significantly reduced ATP hydrolysis ability.[20] Interestingly, the integrity of D107 is required for AMP–AlF$_x$-dependent complex formation, but not for ADP–AlF$_x$-dependent complex formation (Table 1). We infer that D107 is probably involved first in γ phosphate coordination and then in hydrolysis *per se*.[16] Mutating D107 would thus affect interaction with the γ phosphate, but not the latter state when the β–γ phosphate bond has been cleaved, as it is no longer involved in nucleotide interaction due to the change in valence of the γ phosphate of ATP after nucleophilic attack. Integrity of E108 is required for formation of ADP- and AMP–AlF$_x$ dependent complexes, consistent with its role in sensing the state of the γ phosphate (either cleaved or noncleaved) and transmitting changes to the σ^{54} interacting L1 loop.[16] Mutation of E108 presumably impairs the ability to detect the γ phosphate, hence affecting complex formation when using either AMP–AlF$_x$ or ADP–AlF$_x$ (Table 1). Importantly, to relay the state of the γ phosphate in one subunit to the remaining hexameric assembly, thereby enabling hydrolysis, ^{t}R162 contributes to formation of the catalytic centre in the neighbouring subunit. Since the integrity of R162 is required for AMP–AlF$_x$- but not ADP–AlF$_x$-dependent complex formation, we propose that ^{t}R162 is also involved in γ phosphate coordination and catalysis. As integrity of R168 is required for both AMP–AlF$_x$- and ADP–AlF$_x$-dependent complex formation, ^{t}R168 is probably involved in interactions with other parts of the nucleotide (namely, the C_2' and C_3' hydroxyl groups), acting as a nucleotide-dependent self-association determinant rather than a catalytic residue *per se*.[14] It is interesting to note that we were unable to identify a mutation that supports formation of a stable AMP–AlF$_x$ complex and not an ADP–AlF$_x$ complex.

In this study, we identified and characterised a new nucleotide analogue supporting formation of a stable bEBP•σ^{54} (Eσ^{54}) complex. In the crystal structure of PspF$_{1–275}$•AMP–AlF$_x$ we observe an extra density (probably due to the AlF$_x$ moiety) linked to the AMP moiety, which occupies the same position as the γ phosphate in the PspF$_{1–275}$-ATP-bound structure. Furthermore, in the Mg-AMP-bound structure presented here, the α phosphate (of AMP) occupies the same position as the β phosphate of ATP in the PspF$_{1–275}$-ATP-bound structure. These data taken together suggest that occupancy of the α phosphate position is not as important as occupancy of the β phosphate and γ phosphate positions for stimulating stable complex formation. The change in the ribose–phosphate bond observed for AMP (compared to AMPPNP, ATP and ADP) resembles that observed for hGBP1, suggesting a level of conservation between nucleotide-binding pocket properties. We propose that AMP–AlF$_x$ will be a useful tool to study the ATP-binding pockets of AAA$^+$ proteins and, more specifically, to demonstrate how residues of the AAA$^+$ catalytic centre are implicated in nucleotide stabilisation and utilisation. The apparent adaptability of AMP in this complex suggests that AMP–AlF$_x$ could enable identification of new functional states of AAA$^+$ proteins in complex with their natural target. Finally, to our knowledge, this is the first time that AMP–AlF$_x$ has been reported to act as a nucleotide analogue. It can therefore be regarded as a powerful new tool to study the mechanisms of other AAA$^+$ protein family members and, more generally, Walker motif ATPases.

Acknowledgements

We thank Dr P. Burrows for comments on the manuscript. We are grateful to members of Prof. Buck's and Dr Zhang's laboratories for helpful discussions and friendly support. This work was supported by grants from the Biotechnology and Biological Sciences Research Council and Wellcome Trust to M.B. and X.Z. M.B. acknowledges fellowship support from the Leverhulm trust. N.J. was the recipient of a European Molecular Biology Organization fellowship (ALTF 387-2005). Coordinates for the reported structure have been deposited in the Protein Data Bank with accession code 2VII.

References

1. Rappas, M., Bose, D. & Zhang, X. (2007). Bacterial enhancer-binding proteins: unlocking sigma(54)-dependent gene transcription. *Curr. Opin. Struct. Biol.* **17**, 110–116.

2. Schumacher, J., Joly, N., Rappas, M., Zhang, X. & Buck, M. (2006). Structures and organisation of AAA+ enhancer binding proteins in transcriptional activation. *J. Struct. Biol.* **156**, 190–199.
3. Wigneshweraraj, S. R., Burrows, P. C., Bordes, P., Schumacher, J., Rappas, M., Finn, R. D. *et al.* (2005). The second paradigm for activation of transcription. *Prog. Nucleic Acid Res. Mol. Biol.* **79**, 339–369.
4. Wedel, A., Weiss, D. S., Popham, D., Droge, P. & Kustu, S. (1990). A bacterial enhancer functions to tether a transcriptional activator near a promoter. *Science*, **248**, 486–490.
5. Bordes, P., Wigneshweraraj, S. R., Chaney, M., Dago, A. E., Morett, E. & Buck, M. (2004). Communication between Esigma(54), promoter DNA and the conserved threonine residue in the GAFTGA motif of the PspF sigma-dependent activator during transcription activation. *Mol. Microbiol.* **54**, 489–506.
6. Bordes, P., Wigneshweraraj, S. R., Schumacher, J., Zhang, X., Chaney, M. & Buck, M. (2003). The ATP hydrolyzing transcription activator phage shock protein F of *Escherichia coli*: identifying a surface that binds sigma 54. *Proc. Natl. Acad. Sci. USA*, **100**, 2278–2283.
7. Lee, S. Y., De La Torre, A., Yan, D., Kustu, S., Nixon, B. T. & Wemmer, D. E. (2003). Regulation of the transcriptional activator NtrC1: structural studies of the regulatory and AAA+ ATPase domains. *Genes Dev.* **17**, 2552–2563.
8. Rappas, M., Schumacher, J., Beuron, F., Niwa, H., Bordes, P., Wigneshweraraj, S. *et al.* (2005). Structural insights into the activity of enhancer-binding proteins. *Science*, **307**, 1972–1975.
9. Sallai, L. & Tucker, P. A. (2005). Crystal structure of the central and C-terminal domain of the sigma(54)-activator ZraR. *J. Struct. Biol.* **151**, 160–170.
10. De Carlo, S., Chen, B., Hoover, T. R., Kondrashkina, E., Nogales, E. & Nixon, B. T. (2006). The structural basis for regulated assembly and function of the transcriptional activator NtrC. *Genes Dev.* **20**, 1485–1495.
11. Chaney, M., Grande, R., Wigneshweraraj, S. R., Cannon, W., Casaz, P., Gallegos, M. T. *et al.* (2001). Binding of transcriptional activators to sigma 54 in the presence of the transition state analog ADP–aluminum fluoride: insights into activator mechanochemical action. *Genes Dev.* **15**, 2282–2294.
12. Chen, B., Doucleff, M., Wemmer, D. E., De Carlo, S., Huang, H. H., Nogales, E. *et al.* (2007). ATP ground- and transition states of bacterial enhancer binding AAA+ ATPases support complex formation with their target protein, sigma54. *Structure*, **15**, 429–440.
13. Wittinghofer, A. (1997). Signaling mechanistics: aluminum fluoride for molecule of the year. *Curr. Biol.* **7**, R682–R685.
14. Rappas, M., Schumacher, J., Niwa, H., Buck, M. & Zhang, X. (2006). Structural basis of the nucleotide driven conformational changes in the AAA+ domain of transcription activator PspF. *J. Mol. Biol.* **357**, 481–492.
15. Joly, N., Schumacher, J. & Buck, M. (2006). Heterogeneous nucleotide occupancy stimulates functionality of phage shock protein F, an AAA+ transcriptional activator. *J. Biol. Chem.* **281**, 34997–35007.
16. Joly, N., Rappas, M., Wigneshweraraj, S. R., Zhang, X. & Buck, M. (2007). Coupling nucleotide hydrolysis to transcription activation performance in a bacterial enhancer binding protein. *Mol. Microbiol.* **66**, 583–595.
17. Cannon, W., Bordes, P., Wigneshweraraj, S. R. & Buck, M. (2003). Nucleotide-dependent triggering of RNA polymerase–DNA interactions by an AAA regulator of transcription. *J. Biol. Chem.* **278**, 19815–19825.
18. Emsley, P. & Cowtan, K. (2004). Coot: model-building tools for molecular graphics. *Acta Crystallogr., Sect. D: Biol. Crystallogr.* **60**, 2126–2132.
19. Ghosh, A., Praefcke, G. J., Renault, L., Wittinghofer, A. & Herrmann, C. (2006). How guanylate-binding proteins achieve assembly-stimulated processive cleavage of GTP to GMP. *Nature*, **440**, 101–104.
20. Hanson, P. I. & Whiteheart, S. W. (2005). AAA+ proteins: have engine, will work. *Nat. Rev. Mol. Cell. Biol.* **6**, 519–529.